

# Physiological tracer distribution and benign lesion incidental uptake of Al<sup>18</sup>F-NOTA-FAPI-04 on PET/CT imaging

Ying Kou<sup>a,\*</sup>, Xuemei Jiang<sup>a,\*</sup>, Yutang Yao<sup>a</sup>, Jiaqi Shen<sup>a</sup>, Xiao Jiang<sup>a,b</sup>, Shirong Chen<sup>a</sup>, Hao Lu<sup>a</sup>, Xiaoxiong Wang<sup>a</sup>, Meng Zhao<sup>a</sup>, Dingqiong Xiao<sup>a</sup>, Taipeng Shen<sup>a</sup>, Wei Zhang<sup>a</sup> and Zhuzhong Cheng<sup>a</sup>

**Objective** To systematically investigate the physiological distribution and benign lesion incidental uptake of Al<sup>18</sup>F-NOTA-FAPI-04 (<sup>18</sup>F-FAPI) in cancer patients to establish the normal uptake range in relevant organs and lesions.

**Methods** Twenty patients who underwent <sup>18</sup>F-FAPI PET/CT imaging were retrospectively assessed. Organ and benign lesion tracer uptake was quantified based on standardized uptake values (SUVmax and SUVmean). We compared the variation in tracer uptake in certain organs between men and women, analyzed the possible reasons for diffuse uptake in the thyroid, and assessed tracer uptake variations in the uterus in different menstrual cycle phases. Incidental tracer uptake in benign lesions was also assessed.

**Results** Physiological <sup>18</sup>F-FAPI uptake was observed in the urinary tract, biliary tract system, submandibular glands, pancreas, thyroid, uterus, intestine, prostate gland, parotid gland, myocardium, kidney cortex, and muscles, but not the brain, lungs, liver, spleen, colon, and breasts. The SUVmean for each organ was similar for women and men (all  $P > 0.05$ ). Diffuse tracer uptake in the thyroid was caused by normal thyroid or thyroiditis; there were no statistically significant differences between them (SUVmax:  $t = -1.3$ ,  $P = 0.25$ ; SUVmean:  $t = -1.1$ ,  $P =$

0.31). There was a significant difference for uterus uptake among different menstrual cycle phases (SUVmax:  $F = 5.08$ ,  $P = 0.04$ ; SUVmean:  $F = 5.19$ ,  $P = 0.04$ ). Incidental benign lesion tracer uptake was observed in patients with esophagitis, thyroiditis, arthritis, fractures, and uterine fibroids.

**Conclusion** This study provides a reference range for <sup>18</sup>F-FAPI uptake in relevant organs and benign lesions. Benign lesion <sup>18</sup>F-FAPI uptake may reduce <sup>18</sup>F-FAPI PET/CT specificity. *Nucl Med Commun* XXX: 000–000 Copyright © 2022 Wolters Kluwer Health, Inc. All rights reserved.

Nuclear Medicine Communications XXX, XXX:000–000

**Keywords:** Al<sup>18</sup>F-NOTA-FAPI-04, benign lesions, biodistribution, incidental uptake, PET/CT

<sup>a</sup>The PET/CT Center, Department of Nuclear Medicine, Sichuan Cancer Hospital and Institute, Sichuan Cancer Center, School of Medicine, University of Electronic Science and Technology of China, Chengdu, Sichuan, People's Republic of China and <sup>b</sup>Institute of Isotope, China Institute of Atomic Energy, Beijing, China

Correspondence to Zhuzhong Cheng, MD, The PET/CT Center, Department of Nuclear Medicine, Sichuan Cancer Hospital and Institute, Sichuan Cancer Center, School of Medicine, University of Electronic Science and Technology of China, No.55, Section 4, South People's Road, Chengdu, Sichuan 610041, People's Republic of China  
Tel: +86 15228880392; e-mail: K1249987063@126.com

\*Ying Kou and Xuemei Jiang contributed equally to the writing of this article.

Received 19 January 2022 Accepted 29 March 2022

## Introduction

The formation of supporting tumor stroma is required when the size of a tumor lesion exceeds 1–2 mm, and this stroma eventually comprises a major part of the lesion [1–3]. Cancer-associated fibroblasts are an important component of tumor stroma; they are present in more than 90% of epithelial carcinomas, and differ from normal fibroblasts because they overexpress fibroblast activation protein (FAP) [4,5]. Based on this characteristic, many small-molecule inhibitors of FAP (FAPis) labeled with radioactive tracers (<sup>68</sup>Ga, <sup>18</sup>F, or <sup>177</sup>Lu) have been synthesized as theranostic radiotracers for cancer. Previous studies have demonstrated that FAPI PET/computed tomography (CT) performs well in cases of epithelial tumors, including those in the breasts, pancreas, and gastrointestinal tract, because of their excellent tumor uptake and high sensitivity for detecting lesions [6–11]. Other types of cancer, such as sarcomas and lymphomas,

have also been well imaged using FAPI PET/CT [12–17]. Therefore, FAPis may emerge as promising alternatives to fluorodeoxyglucose (FDG) for tumor imaging, and it has even been proposed that FAPI PET/CT might replace FDG PET/CT in the next decade [2].

Nevertheless, although FAPI PET/CT tumor imaging has shown promising preclinical and clinical results, several pitfalls have appeared with the extension of its applications and related research, especially with regard to nonspecific FAPI uptake. Many studies have demonstrated that FAPI is not tumor-specific and that various benign tumors and non-neoplastic disease entities may have FAPI uptake [18–20]. However, there is very little data on the use of FAPI PET/CT for differentiating between cancer and physiologic reactions or benign diseases, because there have been very few studies on the intrinsic variability of physiological FAPI distribution

[21]. Moreover, many studies on physiological FAPI distribution have focused on the  $^{68}\text{Ga}$  radionuclide rather than  $^{18}\text{F}$  [5,21,22]. As  $^{18}\text{F}$ -labeled FAPI has more favorable physical properties, high production capacity and good imaging characteristics, it may be an ideal agent for PET imaging.

Therefore, in this study, we investigated the physiological distribution and benign lesion incidental uptake of  $\text{Al}^{18}\text{F}$ -NOTA-FAPI-04 ( $^{18}\text{F}$ -FAPI) in patients and established the range of normal uptake in organs and lesions with the aim of reducing the probability of misdiagnosis and identifying appropriate clinical applications.

## Methods

### Patients

This retrospective study was approved by the ethics committee of Sichuan Cancer Hospital (SCCHEC-04-2020-001). Twenty patients with suspected or diagnosed cancer underwent  $^{18}\text{F}$ -FAPI PET/CT for tumor staging or diagnosis in our department between July 2020 and July 2021. Informed consent was obtained from each participant prior to  $^{18}\text{F}$ -FAPI PET/CT imaging. All patients were older than 18 years of age and were able to provide written informed consent. For investigation regarding the reason for diffuse thyroid  $^{18}\text{F}$ -FAPI uptake, the patients underwent cervical ultrasound, thyroid function testing (for FT3, FT4, TSH, TgAb, TPOAb), and other laboratory tests or imaging if necessary. None of the women included in this study were pregnant.

### Radiosynthesis and quality control

The detailed process of radiosynthesis has been described previously [23]. The AllinOne module (Trasis, Ans, Belgium) was modified for automatic synthesis of  $^{18}\text{F}$ -FAPI. Briefly,  $^{18}\text{F}$ - was acquired on-site using a Sumitomo HM-10 cyclotron system (Sumitomo Heavy Industries, Tokyo, Japan) by irradiation of  $[\text{O}^{18}]\text{H}_2\text{O}$  with 10 MeV protons, and reacted with 0.15 mg NOTA-FAPI-04 (Paite Biotech, Beijing, China) at  $130^\circ\text{C}$  for 8 min at a pH of 4.0. The purified products were then collected using an HLB cartridge (waters corporation). HPLC (Shimadzu LC-15, Suzhou, China) was performed to test the quality of the final  $^{18}\text{F}$ -FAPI product, with a radiochemical purity exceeding 95% required for the product to qualify. Further physical and biological quality controls (for appearance, color, pH, etc.) were performed in compliance with current pharmacopoeias.

### $^{18}\text{F}$ -FAPI PET/computed tomography scanning

There was no special preparation for patients on the day of  $^{18}\text{F}$ -FAPI PET/CT scanning. Scanning was performed using a Biograph mCT-64 scanner (Siemens, Germany) about 60 min after intravenous injection of  $^{18}\text{F}$ -FAPI (mean activity:  $8.8 \pm 0.9$  mCi; range: 7.1–10.6 mCi). Each patient first underwent low-dose (1.3–1.5

mSv) CT from the vertex to the mid-thigh (with standard CT parameters: 140 keV, 42 mAs, slice thickness: 5 mm, pitch: 0.8). Subsequently, a PET scan was performed with the same scan scope as that used for low-dose CT. The need for focal diagnostic CT was assessed based on the diagnostic demands. The PET data were acquired in a 3D-Flow-Motion with an acquisition time of 2 min per bed position. The acquired data were reconstructed using an ordered subset expectation maximization iterative reconstruction algorithm (three iterations, 21 subsets). Patients were requested to self-report any abnormalities up to 30 min after the end of the examination.

### Image analysis, uptake values, and study groups

All images were evaluated by two board-certified nuclear medicine physicians experienced in assessing PET/CT images; any disagreements were resolved by consensus. The intensity of  $^{18}\text{F}$ -FAPI uptake in organs or benign lesions was quantified in terms of the standardized uptake value (SUV) (SUVmax, and SUVmean). SUVs were acquired by measuring the volume of interest in a 1- or 2-cm spherical region drawn in the parenchyma of organs and benign lesions, according to the size of the organ and 42% threshold isocontour [24,25]. Blood pool SUV was acquired by drawing a 1-cm spherical region in the center of the descending thoracic aorta, excluding the aortic wall. Disease lesions were not included in the organ volumes of interest.

We defined an organ as having  $^{18}\text{F}$ -FAPI uptake when the SUVmax of that organ was higher than that of the blood pool (SUVmax = 1.6); on the contrary, an organ was deemed to have no  $^{18}\text{F}$ -FAPI uptake when its SUVmax was less than that of the blood pool. Benign lesions were confirmed based on other imaging methods or serology or pathological results (if available), and incidental tracer uptake in benign lesions was defined as the presence of foci with increased  $^{18}\text{F}$ -FAPI uptake compared to that of the surrounding lesion tissue.

Cases of diffuse  $^{18}\text{F}$ -FAPI uptake in the thyroid were categorized into either the thyroiditis or normal group depending on thyroid imaging, thyroid function, and other laboratory test results. Patients in the thyroiditis group exhibited evidence of subacute thyroiditis, Hashimoto thyroiditis, or autoimmune thyroiditis based on serology and/or imaging, whereas those in the normal group had no abnormality with regard to serology, imaging, or clinical symptoms.

The menstrual cycle is divided into the follicular and luteal phases. The follicular phase begins with the onset of menses and ends on the day before the luteinizing hormone surge. The luteal phase begins on the day of the luteinizing hormone surge and ends at the next onset of menses. Menopause was defined as a period of at least 12 months without a menstrual cycle.

**Statistical analysis**

Statistical analysis was performed using SPSS (version 22.0; IBM). The SUVmax and SUVmean in relevant organs and lesions are presented in terms of the mean ± SD. The individual organ SUVmax and SUVmean values in men and women were compared using the *t*-test (for normally distributed populations) or *t*'-test (for non-normally distributed populations), which was similar to the analysis of diffuse thyroid uptake. Differences in <sup>18</sup>F-FAPI uptake in the uterus in different menstrual cycle phases were compared using one-way analysis of variance, and LSD or Tamhane's T2 method according to homogeneity of variance was needed to analyze the difference between any two menstrual cycle phases. A *P*-value <0.05 was considered statistically different.

**Results**

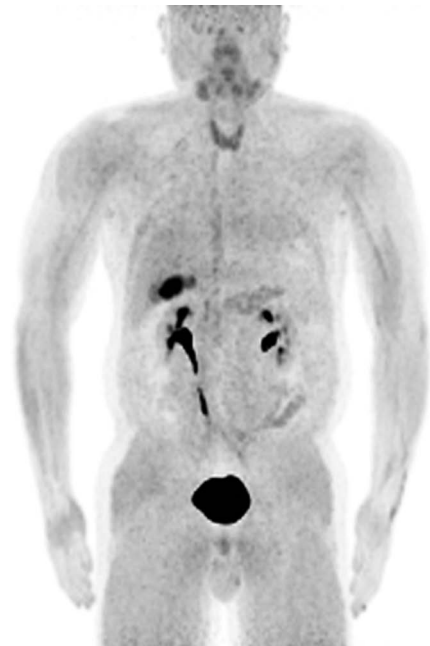
**Study population**

Twenty patients (11 women and nine men) were included in this study. The median age of the patients was 46 years (range, 24–66 years). Seven types of cancers were detected: lung cancer (*n* = 2), lymphoma (*n* = 3), gastric cancer (*n* = 1), breast cancer (*n* = 1), glioma (*n* = 8), liver cancer (*n* = 2), and nasopharyngeal carcinoma (*n* = 3).

**Physiological distribution of <sup>18</sup>F-FAPI in healthy organs**

The <sup>18</sup>F-FAPI uptake variability in healthy organs is presented in Table 1. Physiological tracer uptake was observed in the urinary tract, biliary tract system, submandibular glands, pancreas, thyroid, uterus, intestine, prostate gland, parotid gland, myocardium, kidney cortex, and muscles (Fig. 1), but not in the brain, lungs, liver, spleen, colon, and breasts. <sup>18</sup>F-FAPI uptake was highest (SUVmax ≥ 8) in the urinary tract, biliary tract system, and uterus. The submandibular glands, pancreas, thyroid, parotid gland, and intestine showed moderate <sup>18</sup>F-FAPI uptake (SUVmax: 3.0–8.0), while mild <sup>18</sup>F-FAPI uptake

Fig. 1.



Physiological tracer distribution in a man. The urinary tract, biliary tract system, submandibular glands, pancreas, and thyroid showed strong <sup>18</sup>F-FAPI accumulation.

(SUVmax: 1.6–3.0) was observed in the myocardium, kidney cortex, muscles, and prostate gland.

Regarding variations in SUVmax and SUVmean in different organs between men and women, there were no significant differences in terms of both SUVmean and SUVmax (*P* > 0.05), except in the kidney cortex – the SUVmax of the male kidney cortex was slightly higher than that in females (2.7 ± 0.4 vs. 2.3 ± 0.3, *t* = -2.69, *P* = 0.02; Table 2).

**Uptake in thyroid**

All patients had diffuse <sup>18</sup>F-FAPI uptake in the thyroid (average SUVmax and SUVmean: 5.7 ± 3.6 and 3.6 ± 2.2, respectively). Of the 20 patients, only seven underwent cervical ultrasound and thyroid function examination (FT3, FT4, TSH, TgAb, TPOAb); four of these patients were diagnosed with thyroiditis. A comparison of thyroid tracer uptake between the thyroiditis and normal thyroid groups showed that the thyroid SUVmax (*t* = -1.3, *P* = 0.25) and SUVmean (*t* = -1.1, *P* = 0.31) of both groups were similar (Table 3).

**Uptake in the uterus in different phases of the menstrual cycle**

As the uterus is a hormone-sensitive organ, we compared its <sup>18</sup>F-FAPI uptake in different menstrual cycle phases (Table 4). As the menstrual cycle phase of one patient was not known, only 10 women were included

Table 1. Average SUVmax and SUVmean of each organ with physiological tracer uptake

Organ	SUVmax ± SD	SUVmean ± SD
Brain	0.3 ± 0.1	0.2 ± 0.1
Parotid gland	3.0 ± 1.0	2.0 ± 0.6
Submandibular glands	6.1 ± 1.8	4.1 ± 1.1
Thyroid	5.7 ± 3.6	3.6 ± 2.2
Lungs	1.0 ± 0.2	0.6 ± 0.2
Myocardium	2.1 ± 0.6	1.5 ± 0.3
Blood pool	1.6 ± 0.2	1.4 ± 0.2
Liver	1.6 ± 0.4	0.9 ± 0.3
Gallbladder	19.4 ± 8.8	12.4 ± 5.9
Bile ducts	8.8 ± 4.2	5.7 ± 2.8
Pancreas	4.7 ± 1.5	2.9 ± 1.0
Spleen	1.3 ± 0.3	0.8 ± 0.2
Kidney cortex	2.4 ± 0.4	1.8 ± 0.4
Colon	1.3 ± 0.3	0.8 ± 0.3
Muscles	2.2 ± 0.3	1.6 ± 0.3
Intestine	5.7 ± 1.8	3.3 ± 1.0
Breasts	1.6 ± 1.3	1.0 ± 0.8
Uterus	11.8 ± 7.7	7.3 ± 4.7
Prostate gland	2.8 ± 0.6	1.9 ± 0.4
Bladder	56.9 ± 41.2	38.3 ± 29.1

**Table 2. The variation of the SUVmax and SUVmean between females and males**

Organ	SUVmax $\pm$ SD (F)	SUVmax $\pm$ SD (M)	t(t')	P values	SUVmean $\pm$ SD (F)	SUVmean $\pm$ SD (M)	t(t')	P values
Parotid gland	2.8 $\pm$ 1.2	3.2 $\pm$ 0.9	-0.1	0.32	1.9 $\pm$ 0.8	2.2 $\pm$ 0.4	-0.1	0.33
SMG	5.7 $\pm$ 1.4	6.6 $\pm$ 2.2	-1.1	0.29	3.7 $\pm$ 0.8	4.4 $\pm$ 1.3	-1.45	0.16
Myocardium	2.0 $\pm$ 0.3	2.3 $\pm$ 0.7	-1.28	0.23	1.3 $\pm$ 0.2	1.4 $\pm$ 0.4	-0.77	0.45
Gallbladder	21.3 $\pm$ 8.0	16.6 $\pm$ 9.8	1.08	0.3	13.9 $\pm$ 5.5	10.2 $\pm$ 6.2	1.29	0.22
Common bile duct	8.9 $\pm$ 4.6	8.7 $\pm$ 3.9	0.07	0.94	5.5 $\pm$ 2.8	5.9 $\pm$ 3.2	-0.25	0.8
Pancreas	4.9 $\pm$ 1.6	4.5 $\pm$ 1.5	0.52	0.61	3.1 $\pm$ 1.0	2.8 $\pm$ 1.0	0.67	0.51
Kidney	2.3 $\pm$ 0.3	2.7 $\pm$ 0.4	-2.69	0.02	2.0 $\pm$ 0.4	1.8 $\pm$ 0.5	1.1	0.23
Muscles	2.2 $\pm$ 0.2	2.2 $\pm$ 0.4	-0.43	0.67	1.6 $\pm$ 0.3	1.5 $\pm$ 0.3	0.29	0.77
Intestine	5.7 $\pm$ 1.8	0	-	-	3.3 $\pm$ 1.0	0	-	-
Bladder	64.6 $\pm$ 48.1	47.4 $\pm$ 33.2	0.94	0.36	43.5 $\pm$ 34.5	31.8 $\pm$ 21.0	0.89	0.39

SMG, submandibular glands.

**Table 3. The variation of the SUVmax and SUVmean in thyroid between thyroiditis and normal thyroid**

	Thyroiditis	Normal thyroid	t	P values
SUVmax $\pm$ SD	4.6 $\pm$ 0.8	6.4 $\pm$ 2.8	-1.3	0.25
SUVmean $\pm$ SD	2.7 $\pm$ 1.1	3.8 $\pm$ 1.6	-1.1	0.31

**Table 4. The  $^{18}\text{F}$ -FAPI uptake of uterus in different menstrual cycle phases**

	Follicular phase	Luteal phase	Menopause	F	P values
Uterus SUVmax $\pm$ SD	12.9 $\pm$ 6.3	18.0 $\pm$ 7.8	4.7 $\pm$ 2.4	5.08	0.04
Uterus SUVmean $\pm$ SD	8.3 $\pm$ 4.3	10.9 $\pm$ 4.5	2.8 $\pm$ 1.3	5.19	0.04

**Table 5. The incidental  $^{18}\text{F}$ -FAPI uptake (SUVmax and SUVmean) of benign lesions**

Localization	SUVmax ( $\pm$ SD)	SUVmean ( $\pm$ SD)
Oesophagitis	4.4	3.0
Thyroiditis	4.6 $\pm$ 0.8	2.7 $\pm$ 1.1
Arthritis	6.1	3.6
Old rib fracture	3.1	1.9
Uterine fibroids	6.8	4.8

in the final analysis. Three patients were in the follicular phase, three patients were in the luteal phase, and four patients were in menopause.  $^{18}\text{F}$ -FAPI uptake in the uterus was found to be lowest in the menopausal patients; moreover, there was a significant difference for uterus uptake among different menstrual cycle phases either for SUVmax ( $F = 5.09$ ,  $P = 0.04$ ) or SUVmean ( $F = 5.19$ ,  $P = 0.04$ ). Furthermore, we found that  $^{18}\text{F}$ -FAPI uptake in the uterus was higher in the luteal phase than that in menopause ( $P = 0.02$ ), while uptake in the follicular phase was similar to that in the luteal phase ( $P > 0.05$ ) and in menopause ( $P > 0.05$ ).

#### Incidental tracer uptake in benign lesions

Incidental  $^{18}\text{F}$ -FAPI uptake in benign lesions was less extensive than the physiological tracer uptake in organs (Table 5). Among the 20 patients, mild to moderate  $^{18}\text{F}$ -FAPI uptake was observed in one patient with esophagitis (Fig. 2), 4 patients with thyroiditis (Fig. 3), one patient with arthritis (Fig. 4), one patient with rib fracture (Fig. 5), and one patient with uterine fibroids (Fig. 6).

**Fig. 2.**

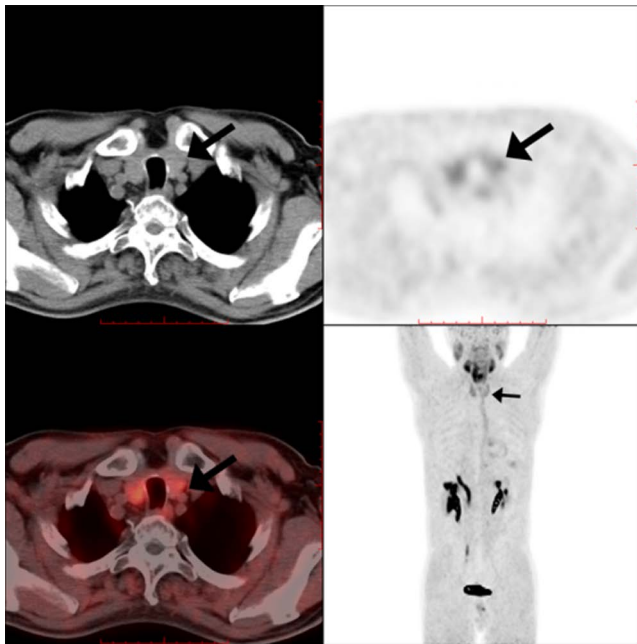
Diffuse tracer uptake was observed in the esophagus (arrows) on  $^{18}\text{F}$ -FAPI PET/CT imaging for a patient with esophagitis.

## Discussion

As FAPI PET/CT is a newer diagnostic tool for cancer imaging than FDG PET/CT, some false-positive diagnoses are not well known. The false-positive results reported till now were mainly from normal organs or benign lesions due to FAPI metabolism, excretion, and physiological expression. Data regarding physiological tracer distribution, intrinsic FAPI uptake variability in normal organs, and benign lesion FAPI uptake will be helpful for radiologists and nuclear medicine physicians to make accurate diagnoses. In this study, we provided a comprehensive assessment of the physiological distribution of  $^{18}\text{F}$ -FAPI and incidental  $^{18}\text{F}$ -FAPI uptake in benign lesions.

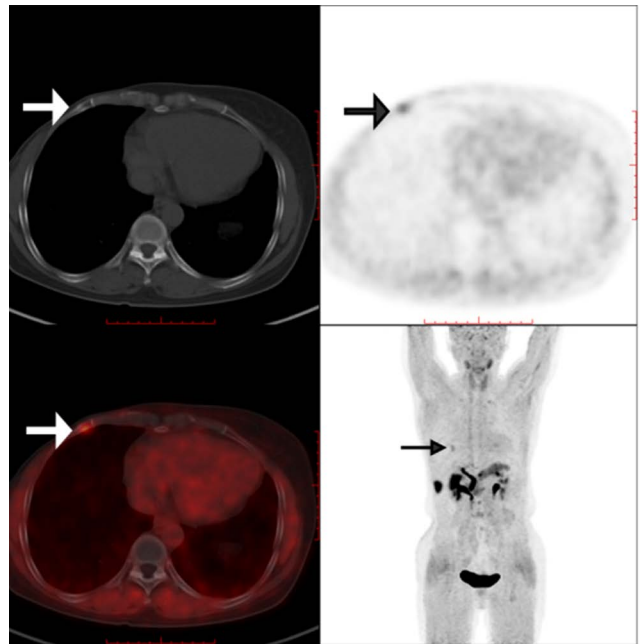
In general, physiological uptake of  $^{18}\text{F}$ -FAPI was observed in the urinary tract, biliary tract system, submandibular

Fig. 3.



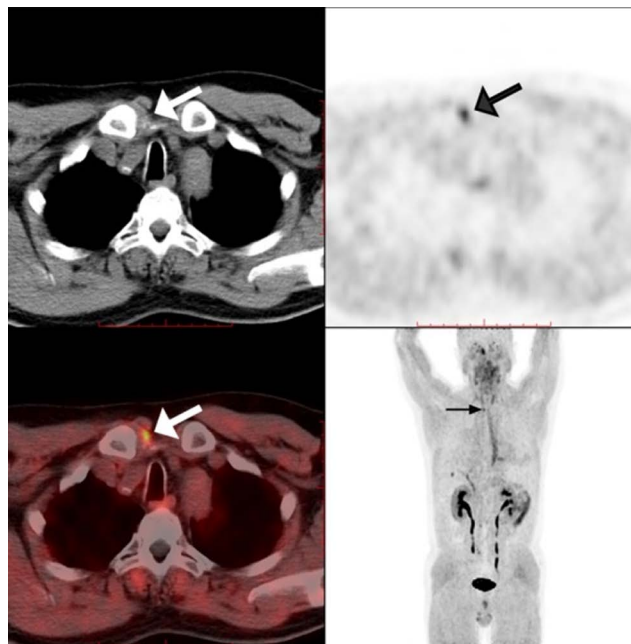
Diffuse tracer uptake was observed in the thyroid (arrows) on  $^{18}\text{F}$ -FAPI PET/CT imaging for a patient with Hashimoto thyroiditis.

Fig. 5.



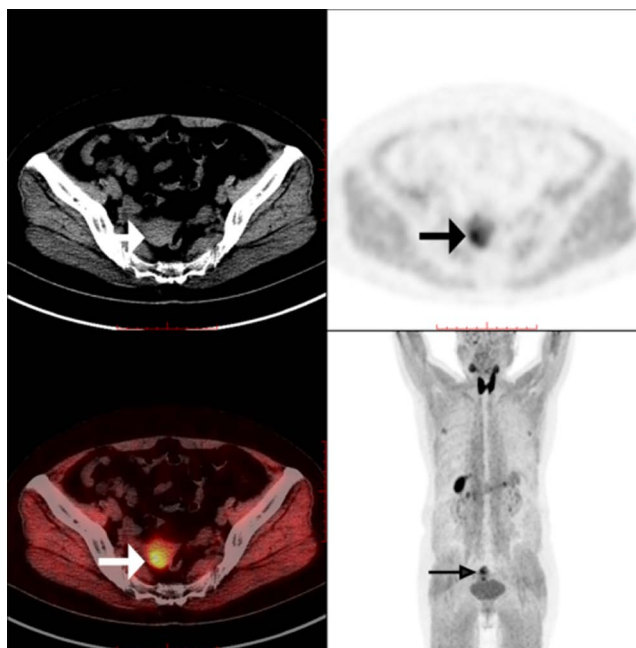
A focal tracer uptake was observed in the right rib for prior rib fracture (arrows) on  $^{18}\text{F}$ -FAPI PET/CT imaging.

Fig. 4.



A focal tracer uptake was observed in the right sternoclavicular joint (arrows) for arthritis on  $^{18}\text{F}$ -FAPI PET/CT imaging.

Fig. 6.



A focal tracer uptake was observed in the lesion of uterine fibroids (arrows) on  $^{18}\text{F}$ -FAPI PET/CT imaging. CT, computed tomography.

glands, pancreas, thyroid, uterus, and intestine, and to a lesser extent, in the myocardium, kidney cortex, muscles, and parotid and prostate glands. Tracer uptake was absent in the brain, lungs, liver, spleen, colon, and breasts. Similar to the study by Wang et al., we found no significant difference between the SUVmean or SUVmax of men and women for any organ [21], except for the SUVmax of the kidney cortex, which was slightly higher in male patients. This may be due to individual differences or statistical errors.

The strong  $^{18}\text{F}$ -FAPI accumulation in the urinary tract and biliary tract system was most probably due to tracer excretion, as our previous animal experiment showed that  $^{18}\text{F}$ -FAPI was excreted by the urinary tract and biliary tract system [23]. The mechanism of excretion of  $^{18}\text{F}$ -FAPI was different from that of  $^{68}\text{Ga}$ -FAPI.  $^{68}\text{Ga}$ -FAPI is a urinary elimination tracer, and thus accumulates in the bladder [25]. High  $^{18}\text{F}$ -FAPI accumulation in the urinary tract and biliary tract system might be a limitation in detecting disease/lesions in these organs.

Apart from the above excretory organs, high  $^{18}\text{F}$ -FAPI uptake was observed in the uterus (mean SUVmax:  $11.8 \pm 7.7$ ), which was similar to that reported by Kessler et al., where the SUVmax of the uterus was 12.2 [26]. Studies have proposed that the high physiological expression of FAP in the uterus could result in FAPI uptake [21,27]. According to one case report, the uterus can show obvious FAPI uptake during the post-pregnancy period and breastfeeding due to increased physiological FAP

expression in the uterus at the special time [28]. As the uterus is a hormone-sensitive organ, we also compared the  $^{18}\text{F}$ -FAPI uptake of the uterus in different menstrual cycle phases. In this study, we found that the most obvious tracer uptake in the uterus was in the luteal phase, followed by the follicular phase, and the postmenopausal stage, which might be related to the upregulation of FAP expression in the luteal uterus and its downregulation in the postmenopausal uterus [26,29]. Furthermore, we found that  $^{18}\text{F}$ -FAPI uptake by the uterus in the luteal phase was higher than that in menopause ( $P = 0.02$ ), while uptake in the follicular and luteal phases was similar.

Subsequently, several glands, such as the submandibular glands, pancreas, and thyroid, showed moderate  $^{18}\text{F}$ -FAPI uptake (SUVmax: 3.0–8.0), which might be related to FAP expression in glandular cells. In accordance with animal experiment results, we also found high  $^{18}\text{F}$ -FAPI uptake in the pancreas and submandibular glands [27]. However, unlike the biodistribution of  $^{68}\text{Ga}$ -FAPI [5],  $^{18}\text{F}$ -FAPI uptake in the pancreas was more obvious, which could reduce the value of  $^{18}\text{F}$ -FAPI PET/CT in diagnosing pancreatic disease.

In this study, we also found that many patients demonstrated diffuse  $^{18}\text{F}$ -FAPI uptake in the thyroid, moreover, tracer uptake between the normal thyroid and thyroiditis groups did not differ significantly. Previous studies have demonstrated that diffuse FAPI uptake in the thyroid is due to thyroiditis, and FAP expression has been immunohistochemically confirmed in autoimmune thyroiditis

[28,30–32]. However, our results indicate that the normal thyroid can also demonstrate intense diffuse FAPI uptake, and we could not differentiate thyroiditis from normal thyroid based on the SUV.

Additionally, the intestine also showed moderate <sup>18</sup>F-FAPI uptake in our cohort, and biliary excretion might be a possible reason for this [22,33].

Compared with the above organs, the myocardium, kidney cortex, muscles, and parotid and prostate glands demonstrated mild <sup>18</sup>F-FAPI uptake, which might be related to the lower FAP expression in the corresponding tissues. The mild muscles <sup>18</sup>F-FAPI uptake (SUV<sub>max</sub> = 2.2 ± 0.3) might also be due to the patients not drinking or being administered furosemide after tracer injection, leading to slow clearance of <sup>18</sup>F-FAPI from muscles.

No tracer uptake (SUV<sub>max</sub> ≤ 1.6) in almost all normal parenchyma of the brain, lungs, liver, spleen, colon, and breasts resulted in excellent visualization of FAPI-avid tumor lesions; thus, <sup>18</sup>F-FAPI PET/CT seems to be quite suitable for imaging tumor lesions in these organs. It should be noted that although the breasts have low FAP expression, they may have moderate or high <sup>18</sup>F-FAPI uptake based on hormonal stimulation [28,34].

Incidental <sup>18</sup>F-FAPI uptake was observed in several benign lesions and in patients with rib fractures, uterine fibroids, esophagitis, thyroiditis, and arthritis. <sup>18</sup>F-FAPI uptake in prior fractures might be due to the fibrotic reactions involved in bone remodeling and reparative processes [35]. <sup>18</sup>F-FAPI uptake in uterine fibroids may be related to FAP overexpression in them. We hypothesized that the increased vascularity and capillary permeability due to inflammatory lesions may result in high perfusion and blood pool effects, manifesting as <sup>18</sup>F-FAPI uptake in such lesions in esophagitis, thyroiditis, and arthritis [26].

There were some limitations to our study, including the retrospective design and small sample size, which might have led to some bias. Nevertheless, this was only a preliminary study, and future studies with larger sample sizes and longer follow-up periods are needed to obtain more reliable conclusions.

**Conclusion**

This study provides a reference range for <sup>18</sup>F-FAPI uptake in normal organs and several types of benign lesions. Our results indicate that benign lesions with <sup>18</sup>F-FAPI uptake might decrease the specificity of <sup>18</sup>F-FAPI PET/CT imaging and that <sup>18</sup>F-FAPI PET/CT might be superior in organs with low background uptake but limited in organs with intense background uptake.

**Acknowledgements**

This study was supported by the Sichuan Science and Technology Project (2019YJ0574 and 2020YFS0421), and

Sichuan Cancer Hospital Outstanding Youth Funding (YB 2021029).

**Conflicts of interest**

There are no conflicts of interest.

**References**

- 1 Moradi F, Iagaru A. Will FAPI PET/CT replace FDG PET/CT in the next decade? Counterpoint-no, not so fast! *AJR Am J Roentgenol* 2021; **216**:307–308.
- 2 Calais J, Mona CE. Will FAPI PET/CT replace FDG PET/CT in the next decade? Point-an important diagnostic, phenotypic, and biomarker role. *AJR Am J Roentgenol* 2021; **216**:305–306.
- 3 Loktev A, Lindner T, Mier W, Debus J, Altmann A, Jäger D, et al. A tumor-imaging method targeting cancer-associated fibroblasts. *J Nucl Med* 2018; **59**:1423–1429.
- 4 Loktev A, Lindner T, Burger EM, Altmann A, Giesel F, Kratochwil C, et al. Development of fibroblast activation protein-targeted radiotracers with improved tumor retention. *J Nucl Med* 2019; **60**:1421–1429.
- 5 Giesel FL, Kratochwil C, Schlittenhardt J, Dendl K, Eiber M, Staudinger F, et al. Head-to-head intra-individual comparison of biodistribution and tumor uptake of <sup>68</sup>Ga-FAPI and <sup>18</sup>F-FDG PET/CT in cancer patients. *Eur J Nucl Med Mol Imaging* 2021; **48**:4377–4385.
- 6 Röhrich M, Naumann P, Giesel FL, Choyke PL, Staudinger F, Wefers A, et al. Impact of <sup>68</sup>Ga-FAPI PET/CT imaging on the therapeutic management of primary and recurrent pancreatic ductal adenocarcinomas. *J Nucl Med* 2021; **62**:779–786.
- 7 Ballal S, Yadav MP, Moon ES, Kramer VS, Roesch F, Kumari S, et al. Biodistribution, pharmacokinetics, dosimetry of [<sup>68</sup>Ga]Ga-DOTA.SA.FAPI, and the head-to-head comparison with [<sup>18</sup>F]F-FDG PET/CT in patients with various cancers. *Eur J Nucl Med Mol Imaging* 2021; **48**:1915–1931.
- 8 Koerber SA, Staudinger F, Kratochwil C, Adeberg S, Haefner MF, Ungerechts G, et al. The role of <sup>68</sup>Ga-FAPI PET/CT for patients with malignancies of the lower gastrointestinal tract: first clinical experience. *J Nucl Med* 2020; **61**:1331–1336.
- 9 Pang Y, Zhao L, Luo Z, Hao B, Wu H, Lin Q, et al. Comparison of <sup>68</sup>Ga-FAPI and <sup>18</sup>F-FDG uptake in gastric, duodenal, and colorectal cancers. *Radiology* 2021; **298**:393–402.
- 10 Kömek H, Can C, Güzel Y, Oruç Z, Gündoğan C, Yildirim ÖA, et al. <sup>68</sup>Ga-FAPI-04 PET/CT, a new step in breast cancer imaging: a comparative pilot study with the <sup>18</sup>F-FDG PET/CT. *Ann Nucl Med* 2021; **35**:744–752.
- 11 Garin-Chesa P, Old LJ, Rettig WJ. Cell surface glycoprotein of reactive stromal fibroblasts as a potential antibody target in human epithelial cancers. *Proc Natl Acad Sci U S A* 1990; **87**:7235–7239.
- 12 Kratochwil C, Flechsig P, Lindner T, Abderrahim L, Altmann A, Mier W, et al. <sup>68</sup>Ga-FAPI PET/CT: tracer uptake in 28 different kinds of cancer. *J Nucl Med* 2019; **60**:801–805.
- 13 Kou Y, Yao Z, Cheng Z. Hepatic lesion of mucosa-associated lymphoid tissue lymphoma revealed by Al<sup>18</sup>F-NOTA-FAPI-04 PET/CT. *Clin Nucl Med* 2022; **47**:e49–e51.
- 14 Dendl K, Finck R, Giesel FL, Kratochwil C, Lindner T, Mier W, et al. FAP imaging in rare cancer entities-first clinical experience in a broad spectrum of malignancies. *Eur J Nucl Med Mol Imaging* 2022; **49**:721–731.
- 15 Kessler L, Ferdinandus J, Hirmas N, Bauer S, Dirksen U, Zarrad F, et al. <sup>68</sup>Ga-FAPI as a diagnostic tool in Sarcoma: data from the <sup>68</sup>Ga-FAPI PET prospective observational trial. *J Nucl Med* 2022; **63**:89–95.
- 16 Koerber SA, Finck R, Dendl K, Uhl M, Lindner T, Kratochwil C, et al. Novel FAP ligands enable improved imaging contrast in sarcoma patients due to FAPI-PET/CT. *Eur J Nucl Med Mol Imaging* 2021; **48**:3918–3924.
- 17 Jin X, Wei M, Wang S, Wang G, Lai Y, Shi Y, et al. Detecting fibroblast activation proteins in lymphoma using <sup>68</sup>Ga-FAPI PET/CT. *J Nucl Med* 2022; **63**:212–217.
- 18 Luo Y, Pan Q, Yang H, Peng L, Zhang W, Li F. Fibroblast activation protein targeted PET/CT with <sup>68</sup>Ga-FAPI for imaging IgG4-related disease: comparison to <sup>18</sup>F-FDG PET/CT. *J Nucl Med* 2021; **62**:266–271.
- 19 Zhou Y, Yang X, Liu H, Luo W, Liu H, Lv T, et al. Value of [<sup>68</sup>Ga]Ga-FAPI-04 imaging in the diagnosis of renal fibrosis. *Eur J Nucl Med Mol Imaging* 2021; **48**:3493–3501.
- 20 Heckmann MB, Reinhardt F, Finke D, Katus HA, Haberkorn U, Leuschner F, Lehmann LH. Relationship between cardiac fibroblast activation protein activity by positron emission tomography and cardiovascular disease. *Circ Cardiovasc Imaging* 2020; **13**:e010628.

- 21 Wang S, Zhou X, Xu X, Ding J, Liu T, Jiang J, *et al.* Dynamic PET/CT imaging of  $^{68}\text{Ga}$ -FAPi-04 in Chinese subjects. *Front Oncol* 2021; **11**:651005.
- 22 Giesel FL, Adeberg S, Syed M, Lindner T, Jiménez-Franco LD, Mavriopoulou E, *et al.* FAPI-74 PET/CT using either  $^{18}\text{F}$ -AIF or Cold-Kit  $^{68}\text{Ga}$  labeling: biodistribution, radiation dosimetry, and tumor delineation in lung cancer patients. *J Nucl Med* 2021; **62**:201–207.
- 23 Jiang X, Wang X, Shen T, Yao Y, Chen M, Li Z, *et al.* FAPI-04 PET/CT using [ $^{18}\text{F}$ ]AIF labeling strategy: automatic synthesis, quality control, and *in vivo* assessment in patient. *Front Oncol* 2021; **11**:649148.
- 24 Zhou X, Li Y, Jiang X, Wang X, Chen S, Shen T, *et al.* Intra-individual Comparison of  $^{18}\text{F}$ -PSMA-1007 and  $^{18}\text{F}$ -FDG PET/CT in the evaluation of patients with prostate cancer. *Front Oncol* 2020; **10**:585213.
- 25 Giesel FL, Kratochwil C, Lindner T, Marschalek MM, Loktev A, Lehnert W, *et al.*  $^{68}\text{Ga}$ -FAPi PET/CT: biodistribution and preliminary dosimetry estimate of 2 DOTA-containing FAP-targeting agents in patients with various cancers. *J Nucl Med* 2019; **60**:386–392.
- 26 Kessler L, Ferdinandus J, Hirmas N, Zarrad F, Nader M, Kersting D, *et al.* Pitfalls and common findings in  $^{68}\text{Ga}$ -FAPi-PET - a pictorial analysis. *J Nucl Med* 2021 [Epub ahead of print]
- 27 Keane FM, Yao TW, Seelk S, Gall MG, Chowdhury S, Poplawski SE, *et al.* Quantitation of fibroblast activation protein (FAP)-specific protease activity in mouse, baboon and human fluids and organs. *FEBS Open Bio* 2013; **4**:43–54.
- 28 Dendl K, Koerber SA, Adeberg S, Röhrich M, Kratochwil C, Haberkorn U, Giesel FL. Physiological FAP-activation in a postpartum woman observed in oncological FAPi-PET/CT. *Eur J Nucl Med Mol Imaging* 2021; **48**:2059–2061.
- 29 Wang LJ, Zhang Y, Wu HB. Intense diffuse uptake of  $^{68}\text{Ga}$ -FAPi-04 in the breasts found by PET/CT in a patient with advanced nasopharyngeal carcinoma. *Clin Nucl Med* 2021; **46**:e293–e295.
- 30 Hotta M, Sonni I, Benz MR, Gafita A, Bahri S, Shuch BM, *et al.*  $^{68}\text{Ga}$ -FAPi-46 and  $^{18}\text{F}$ -FDG PET/CT in a patient with immune-related thyroiditis induced by immune checkpoint inhibitors. *Eur J Nucl Med Mol Imaging* 2021; **48**:3736–3737.
- 31 Zhou Y, He J, Chen Y.  $^{68}\text{Ga}$ -FAPi PET/CT imaging in a patient with thyroiditis. *Endocrine* 2021; **73**:485–486.
- 32 Can C, Gündoğan C, Güzel Y, Kaplan İ, Kömek H.  $^{68}\text{Ga}$ -FAPi uptake of thyroiditis in a patient with breast cancer. *Clin Nucl Med* 2021; **46**:683–685.
- 33 Toms J, Kogler J, Maschauer S, Daniel C, Schmidkonz C, Kuwert T, Prante O. Targeting fibroblast activation protein: radiosynthesis and preclinical evaluation of an  $^{18}\text{F}$ -labeled FAP inhibitor. *J Nucl Med* 2020; **61**:1806–1813.
- 34 Sonni I, Lee-Felker S, Memarzadeh S, Quinn MM, Mona CE, Lückerrath K, *et al.*  $^{68}\text{Ga}$ -FAPi-46 diffuse bilateral breast uptake in a patient with cervical cancer after hormonal stimulation. *Eur J Nucl Med Mol Imaging* 2021; **48**:924–926.
- 35 Qin C, Song Y, Liu X, Gai Y, Liu Q, Ruan W, *et al.* Increased uptake of  $^{68}\text{Ga}$ -DOTA-FAPi-04 in bones and joints: metastases and beyond. *Eur J Nucl Med Mol Imaging* 2022; **49**:709–720.